Received December 19, 2017, accepted February 2, 2018, date of publication February 12, 2018, date of current version March 12, 2018.

Digital Object Identifier 10.1109/ACCESS.2018.2804927

On the Design of OFDMA-Based FFR-Aided Irregular Cellular Networks With Shadowing

JAN GARCÍA-MORALES, (Student Member, IEEE), GUILLEM FEMENIAS, (Senior Member, IEEE), AND FELIP RIERA-PALOU, (Senior Member, IEEE)
Mobile Communications Group, University of the Balearic Islands, 07122 Palma, Spain

Corresponding author: Guillem Femenias (guillem.femenias@uib.es)

This work was supported in part by the Agencia Estatal de Investigación and Fondo Europeo de Desarrollo Regional (AEI/FEDER, UE) under Project ELISA (subproject TEC2014-59255-C3-2-R), in part by the Conselleria d'Educació, Cultura i Universitats (Govern de les Illes Balears) under Grant FPI/1538/2013 (co-financed by the European Social Fund), and in part by the la Caixa Banking Foundation.

ABSTRACT Owing to its high capabilities in terms of spectral efficiency and flexibility, orthogonal frequency division multiple access (OFDMA) has played a crucial role towards the success of 4G cellular systems and an increasing number of actors in the 5G arena strongly advocate for its continuation. OFDMA-based architectures do not introduce intracell interference but, due to the use of very aggressive frequency reuse plans, they must implement some form of inter-cell interference (ICI) control to warrant prescribed levels of quality of service, specially to users located near the cell edge. An efficient technique for mitigating ICI in OFDMA networks is the well-known fractional frequency reuse (FFR) scheme. In FFR, a signal-to-interference-plus-noise ratio threshold is used to categorize mobile stations (MSs) as cell-center or cell-edge MSs. Furthermore, a different number of frequency resources are allocated to cell-center and cell-edge areas according to a prescribed frequency reuse plan. This paper presents an analytical characterization of FFR-aided OFDMA-based multi-cellular networks that, unlike most previous studies, incorporates shadowing effects and, furthermore, considers that base stations are irregularly deployed. This analytical approach can incorporate different scheduling rules and can underpin different designs for which the optimal FFR parameters can be derived. The proposed framework allows the performance evaluation and optimization of any cell in the system by considering the specific network topology, the user association and categorization processes, the spatial density of users and the characteristics of both the fast multipath fading and the spatially correlated slow shadow fading.

INDEX TERMS OFDMA, fractional frequency reuse, irregular networks, correlated shadow fading, optimal threshold, spectral efficiency.

I. INTRODUCTION

Modern cellular wireless communications invariably face two significant impairments, namely, fading and interference. Fading is an inherent phenomenon of radio propagation that can be broadly categorized into large-scale and small-scale. Two distinct sources of fading are deemed to be large-scale: 1) pathloss caused by the distance-related propagation losses, and 2) spatially correlated shadowing caused by the macroscopic characteristics surrounding the transmitter and receiver. Small-scale fading is caused by the multipath propagation and it is usually space, time and frequency dependent (i.e., space/time/frequency-selective). Large-scale fading is tackled by suitably dimensioning the cellular network (i.e., location of base stations (BSs) and transmit power of each BS), whereas orthogonal frequency division multiple access (OFDMA), in combination with scheduling and resource allocation techniques, is the most common approach to counteract the deleterious effects of the selective fading used by the vast majority of current and envisioned wireless standards (e.g., LTE, LTE-A, WiFi, WiMax) [1].

In OFDMA networks, a wideband frequency-selective fading channel is decomposed into a set of orthogonal narrow-band subchannels. These subchannels are jointly used with a time-slotted frame structure to provide a set of frequency/time resource blocks (RBs), which are distributed among cells based on predefined frequency reuse plans. The orthogonality among RBs makes intra-cell interference

negligible. However, due to the common use of high spectral efficiency universal frequency reuse plans with all cells using the same set of RBs, OFDMA-based networks suffer from very high levels of ICI, particularly affecting mobile stations (MSs) located in the cell-edge areas. In order to tackle this problem while aiming at high spectral efficiencies, multiple ICI control (ICIC) strategies have been proposed [2], among which *static* fractional frequency reuse (FFR) and all its variants have been shown to provide a good tradeoff between cell-edge throughput enhancement and overall spectral efficiency [3].

In the downlink of FFR-aided OFDMA-based networks, the channel quality of the set of RBs, typically measured in terms of the signal-to-interference-plus-noise ratio (SINR), varies for different MSs. Such variations in channel conditions can be exploited by using channel-aware schedulers able to allocate each resource block (RB) to an MS with favourable channel conditions at a given scheduling interval. Opportunistic maximum SINR (MSINR) schedulers [4] make the most of the multiuser diversity by allocating the RBs to the MSs experiencing the best channel conditions. In contrast, the round robin (RR) scheduler randomly allocates RBs to MSs in a fair time-sharing approach and without any consideration of channel conditions. In either case, the analytical characterization and optimization of both the cell and network performance are very demanding tasks when irregular cellular deployments affected by correlated shadow fading are considered. Moreover, as the performance of any ICIC strategy is clearly affected by the large scale propagation characteristics perturbing the desired and interfering signals, any simulation-based study must average over many MS positions and multiple possible correlated shadowing realizations, thus making fast and accurate simulations very challenging and time consuming in such environments [5].

A. BACKGROUND WORK

There is a very limited body of literature focusing on tractable analytical models for irregular cellular networks with correlated shadowing. A very interesting approach tackling the performance evaluation of OFDMA-based multi-cellular irregular networks is the one based on the use of stochastic geometry, where both the BSs and MSs are distributed using Poisson Point Processes (PPPs) [6]–[9] (see also references therein). This approach allows characterizing the average performance of the whole set of cellular networks adhering to the properties of the PPP but, unfortunately, it precludes from accurately analyzing the performance of a particular network or an specific cell of a given network. Notice that network/cell-specific performance metrics are crucial to network designers trying to optimize the performance of a planned set of BS locations along with traffic load conditions. Furthermore, practical macrocell deployments, despite being irregular, follow a conscious planning of the BSs, thus its topology lies somewhere in between the idealized hexagonal model and the totally random PPP model.

In contrast to the afore mentioned background work, which relies on the use of stochastic geometry to model the cellular environment, Assaad in [10] and Najjar *et al.* in [11] considered the use of analytical tools to optimize an FFR-based OFDMA regular network. This analytical framework, however, lacked the consideration of both small-scale fading and shadowing and thus, precluded the possibility of analyzing channel-aware scheduling policies. Some of the limitations of these works were overcome in part in [12]–[15], where the presence of small-scale multipath fading and the use of channel-aware schedulers were considered in a mathematically tractable analytical framework. The main drawback of these works, however, was that they only considered the analysis of regularly deployed cellular networks and, furthermore, the presence of (spatially uncorrelated) shadow fading was only taken into account by Xu *et al.* in Monte-Carlo simulation results [12]. Mahmud and Hamdi in [16] proposed a unified framework for the analysis of frequency reuse techniques over composite fading environments and derived tractable analytical expressions for the area spectral efficiency provided by these techniques. However, in this work the authors considered a regular BS deployment, distance-based user association and edge/center user classification, spatially uncorrelated shadow fading and the use of channel-unaware round-robin schedulers. In [17], Alam *et al.* dealt with the shadowing effects to obtain a semi-analytical framework allowing the obtention of energy- and spectral-efficiency trade-offs under different frequency reuse factors. Unfortunately, the framework was, again, only applicable to regular cellular networks and, furthermore, only a single user per cell was considered, this limiting the proposal to resource allocation schemes based on the RR scheduling policy.

B. CONTRIBUTIONS OF THE PAPER

In this paper we present a novel analytical framework allowing the analysis, design and optimization of FFR-aided OFDMA-based irregular cellular networks with spatially correlated shadow fading. The main contributions of this paper can be summarized as follows:

- The mathematical description of the cell association process, one of the main difficulties when trying to derive analytical descriptions of irregular cellular deployments with correlated shadowing is fully characterized for those realistic cases where a MS associates to the BS that, first, belongs to the set of *neighbouring* BSs and, second, provides the MS with the highest average received power.[1]
- Related to the previous contribution, once a MS has been associated to a given BS, the FFR-based resource allocation unit has to decide whether this MS is classified as cell-center or cell-edge. This decision is typically

[1] Assuming that current cellular networks are basically interference limited, a cell association process based on the highest average received power is basically equivalent to a cell association process based on the highest average SINR.

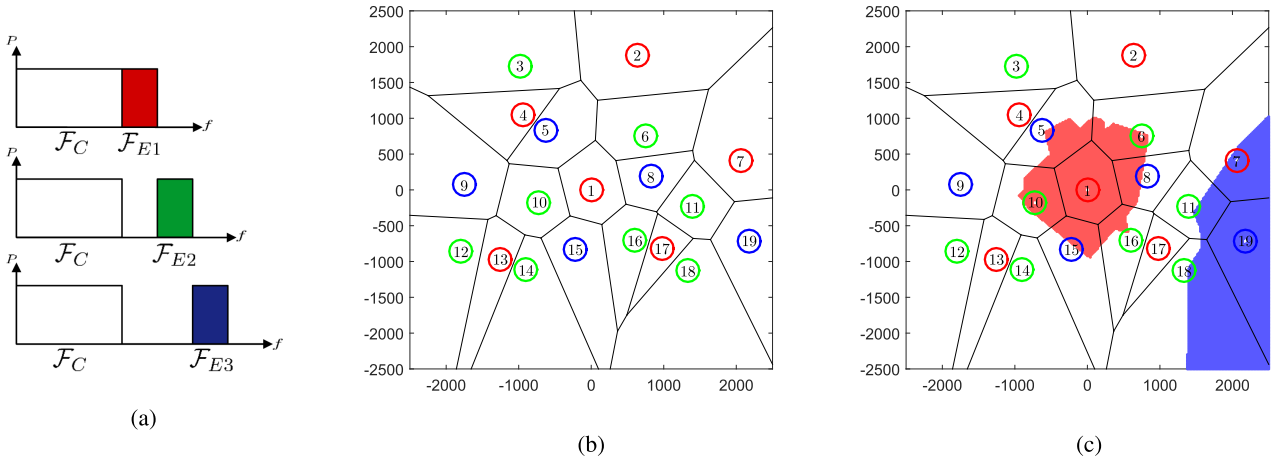

FIGURE 1. Schematic representation of the FFR-aided OFDMA-based irregular cellular network (view of a 5 km × 5 km area, with *simplified* cell boundaries corresponding to a Voronoi tessellation). (a) Frequency subband distributions ($\Delta = 3$). (b) Schematic network topology ($\Delta = 3$). (c) Coverage regions $\mathcal{S}_1$ and $\mathcal{S}_{19}$ with $Q_c = 3$.

based on the average received power experienced by the MS and has to be analytically described using statistical tools. A second contribution of this work is the analytical characterization of the FFR-based user's classification process.

- Cell association and FFR-based user's classification processes are based on the average received power (or equivalently, on the average SINR). The spectral efficiency of the system, however, depends on the behaviour of the instantaneous SINR and, consequently, analyzing the spectral efficiency requires of the statistical characterization of the instantaneous SINR by taking into account both the cell association and the classification of users as either cell-center or cell-edge. Thus, another contribution of this paper is the statistical characterization of the instantaneous SINR experienced by a given user in FFR-aided OFDMA-based irregular cellular networks with spatially correlated shadowing.
- Finally, the statistical characterization of the instantaneous SINR is used to obtain the cell-specific spectral efficiency when using either RR or MSINR scheduling strategies. Furthermore, the proposed analytical framework allows the formulation of optimization problems whose solutions correspond to the FFR-related parameters maximizing the average spectral efficiency of the system. It is worth mentioning that results obtained using the proposed analytical framework have been duly contrasted with results obtained using Monte-Carlo simulations.

C. PAPER ORGANIZATION

The rest of the paper is organized as follows. In Section II the irregular multi-cellular network model under consideration in the context of FFR-aided OFDMA-based networks is introduced. Furthermore. the cell association and FFR-based user classification process are statistically characterized. Section III focuses on the analytical framework used to characterize the instantaneous SINR experienced by MSs under a composite shadow-fading channel. Section IV elaborates on the spectral efficiency performance analysis using both the MSINR and RR scheduling strategies. Optimal designs for the FFR-aided OFDMA-based system are presented in Section V. Extensive analytical and simulation results are provided in Section VI. Finally, the main outcomes of this paper are recapped in Section VII.

II. MULTICELLULAR NETWORK MODEL

A. NETWORK LAYOUT

Let us consider the downlink of an FFR-aided OFDMA-based irregular cellular network such as the one schematically represented in Fig. 1. Located in each cell there is a base station (BS) equipped with an omnidirectional antenna that is serving single-antenna MSs. The locations of the MSs at a given time instant are assumed to follow a stationary Poisson point process (PPP) of normalized intensity λ (measured in MSs per area unit). As a consequence of this assumption, the probability distribution of the number $M_{\mathcal{R}}$ of MSs located within any spatial region $\mathcal{R}$ of area $A_{\mathcal{R}}$ follows a Poisson distribution, that is

$$\Pr\{M_{\mathcal{R}} = M\} = \frac{(\lambda A_{\mathcal{R}})^M e^{-\lambda A_{\mathcal{R}}}}{M!}. \quad (1)$$

The FFR scheme splits each of the cells into both a cell-center and a cell-edge regions. Moreover, aiming at achieving a proper trade-off between network spectral efficiency and throughput fairness among cell-center and cell-edge MSs, the FFR strategy partitions the system bandwidth in such a way that it offers different frequency reuse factors to cell-center and cell-edge MSs. In particular, as shown in Fig. 1a, the total system bandwidth is exploited by means of a set $\mathcal{F}_T$ of N_{RB} RBs (or orthogonal subbands), each with a bandwidth B_{RB} consisting of N_{sc} adjacent subcarriers and small enough to assume that all subcarriers in a subband experience frequency flat fading. The cell-center MSs, particularly immune to co-channel interference, share a set of RBs $\mathcal{F}_C$ on

a universal frequency reuse basis. In contrast, the cell-edge MSs, more prone to intercell interference from neighboring cells, use a frequency reuse factor $\Delta \geq 1$ (a frequency reuse factor of $\Delta = 3$ has been used in Fig. 1b, where the cell-edge regions sharing the same frequency band have been represented using circumferences of the same color) and are allocated non-overlapping equal-size sets of RBs $\mathcal{F}_{E1}$, $\mathcal{F}_{E2}$, ... or $\mathcal{F}_{E\Delta}$ aiming at minimizing the interference among neighboring cells. The total number of RBs in the system is thus given by $N_{\text{RB}} = N_C + \Delta N_E$, where N_C and N_E are the cardinalities of sets $\mathcal{F}_C$ and $\mathcal{F}_{E\delta}$, $\forall \delta \in \{1, \ldots, \Delta\}$, respectively.

B. CELL COVERAGE AREA AND FFR-RELATED CELL REGIONS

In order to ease the visualization, in Fig. 1b the cells have been schematically represented using Voronoi diagrams to partition the coverage area into disjoint regions based on distance minimization to BS locations and, furthermore, the limits between cell-center and cell-edge regions have been represented as circumferences surrounding the BSs. In practice, however, the limits between cells and between cell-center and cell-edge areas are irregular due to the consideration of shadowing.

Every BS in the network transmits a pilot signal and MSs connect to the BS whose pilot signal is received with the highest average power level [1]. As a given MS may not be able to measure the pilot signals from all the BSs in the network, the selection is typically considered to be limited to the nearest Q_c BSs [18]. The selection among the nearest Q_c BSs can also be justified by the use of neighbor cell lists since MSs are regularly provided with a list of handover candidates to be monitored [1]. Let us consider the cell served by a generic BS i, located at Cartesian coordinates $(x^{(i)}, y^{(i)})$, and let us define $\mathcal{S}_i$ as the region containing all the locations having BS i among the Q_c nearest BSs. As an example, Fig. 1c shows the geometry of regions $\mathcal{S}_1$ and $\mathcal{S}_{19}$ containing all the locations having either BS 1 or BS 19 included among the $Q_c = 3$ nearest BSs, respectively. Using previous considerations and definitions, the coverage area of BS i can be safely approximated as the region containing all the locations in $\mathcal{S}_i$ for which the average pilot power level received from BS i is the highest among those received from the Q_c nearest BSs. Hence, from this point onwards the generic region $\mathcal{S}_i$ will be the sample space of the random variables (x_u, y_u) denoting the Cartesian coordinates describing the location of any MS u considered in the performance evaluation of this cell. Obviously, owing to the PPP distribution of MSs on the service area of the cellular network, the coordinates x_u and y_u are uniformly distributed in $\mathcal{S}_i$ and hence, their joint probability density function (PDF) can be expressed as

$$p_{x_u,y_u}(x,y) = \begin{cases} 1/A_{\mathcal{S}_i}, & (x,y) \in \mathcal{S}_i \\ 0, & \text{otherwise}, \end{cases} \tag{2}$$

where recall that $A_{\mathcal{S}_i}$ denotes the area of region $\mathcal{S}_i$.

Average pilot power levels are also used by the FFR scheme to partition each cell in the network into both the cell-center and cell-edge regions. Cell-center and cell-edge regions for BS i contain all locations in $\mathcal{S}_i$ for which the average pilot power level received from BS i is the highest among those received from the Q_c nearest BSs and furthermore, is above or below a power threshold $P_{th}^{(i)}$, respectively. Note that the power threshold is BS-dependent and thus, one of the most important FFR-based network planning parameters will be the set of power thresholds that the different BSs should apply to split the MSs into cell-center and cell-edge groups.

C. CHANNEL MODEL

The channel is subject to path loss, shadowing and small-scale fading. Consequently, assuming that the power transmitted by any BS in the system on any of its frequency/time RBs is equal to P_s (uniform power allocation), the average (with respect to the fast fading) power received by MS u from BS j on a subcarrier belonging to a generic RB (either data or pilot RB) can be expressed as

$$P_{j,u} = P_s L(d_{j,u}) 10^{\varsigma_{j,u}/10}, \tag{3}$$

where $P_s = P_T/(N_{sc}(N_C + N_E))$, $d_{j,u}$ is the distance between BS j and MS u, $L(d_{j,u})$ is the path loss component characterizing the link between BS j and MS u, and $\varsigma_{j,u} \sim \mathcal{N}(0, \sigma_s^2)$ models the shadowing (expressed in dB) between BS j and MS u. Given the statistical characterization of $\varsigma_{j,u}$, it is easy to show that $10^{\varsigma_{j,u}/10}$ follows a lognormal distribution. Furthermore, according to [19], $\varsigma_{j,u}$ can be modelled as a weighted sum of two independent components

$$\varsigma_{j,u} = \sqrt{\epsilon}\, \xi_u + \sqrt{1-\epsilon}\, \nu_{j,u}, \tag{4}$$

where $\xi_u \sim \mathcal{N}(0, \sigma_s^2)$ corresponds to the near field of the uth MS, $\nu_{j,u} \sim \mathcal{N}(0, \sigma_s^2)$ is a BS dependent variable and ϵ is the spatial correlation coefficient related to any pair of BSs. In 3GPP studies, a shadowing correlation coefficient of $\epsilon = 0.5$ between BSs is usually applied [20]. We note that the assumption of identical variances for the whole set of BSs is reasonable as the standard deviation of lognormal shadowing is largely independent of the radio path length [21].

Given the Cartesian coordinates $(x^{(j)}, y^{(j)})$ specifying the location of BS j, the distance between any BS j and MS u, assumed to be located at Cartesian coordinates (x_u, y_u), can be expressed as a function of the random location of the MS as

$$d_{j,u} = \sqrt{\left(x_u - x^{(j)}\right)^2 + \left(y_u - y^{(j)}\right)^2}. \tag{5}$$

Hence, the conditional random variable $P_{j,u}$, conditioned on x_u, y_u and ξ_u, follows a lognormal distribution with a PDF given by

$$f_{P_{j,u}|x_u,y_u,\xi_u}(p|x,y,\xi) = \frac{\varpi/\left(p\sqrt{\pi}\right)}{\sqrt{2(1-\epsilon)}\sigma_s} \exp\left[-\left(\frac{\varpi \ln(p/\overline{P}_{j,u})}{\sqrt{2(1-\epsilon)}\sigma_s}\right)^2\right], \quad p > 0, \tag{6}$$

where $\varpi = 10/\ln(10)$ and $\overline{P}_{j,u} = P_s L(d_{j,u}) 10^{\sqrt{\epsilon}\,\xi_u/10}$. The corresponding cumulative distribution function (CDF) can then be expressed as

$$F_{P_{j,u}|x_u,y_u,\xi_u}(p|x,y,\xi) = \frac{1}{2}\text{erfc}\left(-\frac{\varpi \ln(p/\overline{P}_{j,u})}{\sqrt{2(1-\epsilon)}\sigma_s}\right), \quad p > 0, \tag{7}$$

where erfc(·) denotes the complementary error function.

D. CELL ASSOCIATION AND FFR-BASED USER CLASSIFICATION

As stated in Subsection II-A, MS u is associated to BS i if

$$P_{i,u} = \max_{j\in\Theta_u}\{P_{j,u}\} \triangleq P_{\max,u}, \tag{8}$$

where Θ_u is a set indexing the Q_c nearest BSs to MS u. Additionally, if $P_{i,u} > P_{th}^{(i)}$ then MS u is classified as a cell-center MS and otherwise, it is classified as a cell-edge MS.

From this point onwards, we will use A as a token to represent either the cell-center region C or the cell-edge region E. Let us define the random variable

$$\pi_{i,u}^{A} \triangleq P_{i,u} \quad \text{if } P_{i,u} = P_{\max,u} \quad \text{and } P_L^{(A,i)} \le P_{i,u} \le P_U^{(A,i)}, \tag{9}$$

where $P_L^{(A,i)}$ and $P_U^{(A,i)}$ are used to denote, respectively, the lower and upper received pilot power limits characterizing cell region A of cell i. Taking into account that the set of conditional random variables $\mathcal{P}_u = \{P_{j,u}\}\forall_{j\in\Theta_u}$, conditioned on x_u, y_u and ξ_u, are independent, the conditional PDF of $\pi_{i,u}^{A}$ conditioned on x_u, y_u and ξ_u can be expressed as

$$\begin{aligned} f_{\pi_{i,u}^{A}|x_u,y_u,\xi_u}(p|x,y,\xi) &= f_{P_{i,u}|x_u,y_u,\xi_u}(p|x,y,\xi) \\ &\times \prod_{\substack{j\in\Theta_u \\ j\neq i}} F_{P_{j,u}|x_u,y_u,\xi_u}(p|x,y,\xi) \\ &\times \left[\text{u}\left(p - P_L^{(A,i)}\right) - \text{u}\left(p - P_U^{(A,i)}\right)\right], \end{aligned} \tag{10}$$

with u(·) denoting the unit step function.

The joint PDF of $\pi_{i,u}^{A}$, x_u, y_u and ξ_u, for a generic MS u located in cell-region A of cell i, can be obtained as

$$f_{\pi_{i,u}^{A},x_u,y_u,\xi_u}(p,x,y,\xi) = \frac{f_{\pi_{i,u}^{A}|x_u,y_u,\xi_u}(p|x,y,\xi) f_{\xi_u}(\xi)}{A_{\mathcal{S}_i} P_r^{(A,i)}} \quad \forall\,(x,y)\in\mathcal{S}_i, \tag{11}$$

where $P_r^{(A,i)}$ is the probability that a generic MS $u \in \mathcal{S}_i$ associated to BS i is classified as a MS in cell-region A of cell i, which can be derived as

$$P_r^{(A,i)} = \frac{1}{A_{\mathcal{S}_i}} \int_{-\infty}^{\infty} \iint_{(x,y)\in\mathcal{S}_i} \int_0^{\infty} f_{\pi_{i,u}^{A}|x_u,y_u,\xi_u}(p|x,y,\xi) \times f_{\xi_u}(\xi)\text{d}p\text{d}x\text{d}y\text{d}\xi. \tag{12}$$

The probability that a MS $u \in \mathcal{S}_i$ is associated to BS i is then given by $P_r^{(i)} = P_r^{(C,i)} + P_r^{(E,i)}$.

III. STATISTICAL CHARACTERIZATION OF THE SINR

Using the definition of $\pi_{i,u}^{A}$ in (9), the instantaneous SINR experienced by MS u in cell region A associated to BS i on any of the N_{sc} subcarriers constituting RB $n \in \mathcal{F}_A$ can be expressed as

$$\gamma_{u,n}^{(A,i)} = \frac{\pi_{i,u}^{A}|H_{i,u,n}|^2}{N_0\Delta f + \sum_{j\in\Phi_n^{(A,i)}} P_{j,u}|H_{j,u,n}|^2}, \tag{13}$$

where $H_{j,u,n} \sim \mathcal{N}(0,1)$ is the frequency response resulting from the small-scale fading channel linking the jth BS to MS u on the nth RB during scheduling period t, N_0 is the noise power spectral density, $\Delta f = B_{\text{RB}}/N_{sc}$ is the subcarrier bandwidth, and $\Phi_n^{(A,i)}$ represents the set of BSs interfering MSs served by BS i in cell region A, which is RB-dependent.

The random variables $h_{j,u,n} \triangleq |H_{j,u,n}|^2$ are subject to an exponential distribution $f_h(x) = e^{-x}u(x)$ and thus, its corresponding CDF can be easily obtained as $F_h(x) \triangleq Pr\{h \le x\} = \left(1 - e^{-x}\right)u(x)$. Consequently, the CDF of the instantaneous SINR $\gamma_{u,n}^{(A,i)}$ conditioned on variables $\pi_{i,u}^{A}$, ξ_u, x_u, y_u, the set of small-scale fading gains $\boldsymbol{h}_{u,n} \triangleq \{h_{j,u,n}\}_{j\in\Phi_n^{(A,i)}}$ and the set of shadowing components $\boldsymbol{s}_u \triangleq \{s_{j,u}\}_{j\in\Phi_n^{(A,i)}}$ with $s_{j,u} = 10^{\sqrt{1-\epsilon}\,\nu_{j,u}/10}$, can be derived from (13) as

$$F_{\gamma_{u,n}^{(A,i)}|\pi_{i,u}^{A},x_u,y_u,\xi_u,\boldsymbol{h}_{u,n},\boldsymbol{s}_u}(\gamma|p,x,y,\xi,\boldsymbol{h},\boldsymbol{s}) = 1 - \exp\left[-\frac{\gamma}{p}\left(N_0\Delta f + \sum_{j\in\Phi_n^{(A,i)}} \overline{P}_{j,u}s_j h_j\right)\right], \tag{14}$$

for $\gamma \ge 0$. Now, using the above expression and averaging over the i.i.d. random variables $\boldsymbol{h}_{u,n}$ and $\boldsymbol{s}_u$, the conditional CDF of the instantaneous SINR $\gamma_{u,n}^{(A,i)}$ can be obtained shown in (15), at the top of the next page, where $f_{h_{j,u,n}}(h_j)$ and $f_{j,u}(s_j)$ are the PDFs of variables $h_{j,u,n}$ and $s_{j,u}$, respectively. where $f_{h_{j,u,n}}(h_j)$ and $f_{j,u}(s_j)$ are the PDFs of variables $h_{j,u,n}$ and $s_{j,u}$, respectively.

We can use the change of variables $t_j = \frac{\varpi \ln(s_j)}{\sqrt{2(1-\epsilon)}\sigma_s}$ and the Gauss-Hermite quadrature rule [22] to approximate the expression in(16) as

$$\begin{aligned} F_{\gamma_{u,n}^{(A,i)}|\pi_{i,u}^{A},x_u,y_u,\xi_u}(\gamma|p,x,y,\xi) &= 1 - e^{-\frac{\gamma N_0\Delta f}{p}} \prod_{j\in\Phi_n^{(A,i)}} \int_{-\infty}^{\infty} \frac{e^{-t_j^2}/\sqrt{\pi}}{e^{\frac{\sqrt{2(1-\epsilon)}}{\varpi/(\sigma_s t_j)}}\left(\frac{\gamma\overline{P}_{j,u}}{p}\right) + 1}\text{d}t_j \\ &= 1 - e^{-\frac{\gamma N_0\Delta f}{p}} \prod_{j\in\Phi_n^{(A,i)}} \sum_{l=1}^{N_j} \frac{\omega_{j,l}/\sqrt{\pi}}{e^{\frac{\sqrt{2(1-\epsilon)}\sigma_s t_{j,l}}{\varpi}}\left(\frac{\gamma\overline{P}_{j,u}}{p}\right) + 1}, \end{aligned} \tag{16}$$

for $\gamma \ge 0$, where N_j denotes the number of sample points, $t_{j,l}$ is the lth root of the (physicists version of the) Hermite polynomial $H_{N_j}(x)$, and $w_{j,l}$ is the corresponding weight factor.

$$
\begin{aligned}
&F_{\gamma_{u,n}^{(A,i)}|\pi_{i,u}^{A},x_u,y_u,\xi_u}(\gamma|p,x,y,\xi)\\
&\quad\triangleq Pr\{\gamma_{u,n}^{(A,i)}\le\gamma|\pi_{i,u}^{A}=p,x_u=x,y_u=y,\xi_u=\xi\}\\
&\quad=\int_0^\infty\cdots\int_0^\infty F_{\gamma_{u,n}^{(A,i)}|\pi_{i,u}^{A},x_u,y_u,\xi_u,\boldsymbol{h}_{u,n},\boldsymbol{s}_u}(\gamma|p,x,y,\xi,\boldsymbol{h},\boldsymbol{s})\prod_{j\in\Phi_n^{(A,i)}}f_{h_{j,u,n}}(h_j)f_{s_{j,u}}(s_j)\mathrm{d}h_j\mathrm{d}s_j\\
&\quad=1-\frac{e^{-\gamma N_0\Delta f/p}}{\sqrt{\pi}}\prod_{j\in\Phi_n^{(A,i)}}\int_0^\infty\frac{\varpi/\left(\sqrt{2(1-\epsilon)}\sigma_s\right)}{s_j^2\left(\frac{\gamma\overline{P}_{j,u}}{p}\right)+s_j}\exp\left[-\left(\frac{\varpi\ln(s_j)}{\sqrt{2(1-\epsilon)}\sigma_s}\right)^2\right]\mathrm{d}s_j,\quad\gamma\ge0.
\end{aligned}
\tag{15}
$$

IV. AVERAGE SPECTRAL EFFICIENCY ANALYSIS

Let $\gamma_n^{(A,i)}$ denote the SINR experienced by a generic MS in cell region A that has been scheduled for transmission on RB n. Our goal is to determine the average spectral efficiency on this RB given by

$$
\begin{aligned}
\overline{\eta}_n^{(A,i)}&\triangleq\mathbb{E}_{\gamma_n^{(A,i)}}\left\{\log_2(1+\gamma_n^{(A,i)})\right\}\\
&=\sum_{M=1}^{\infty}\Pr\left\{M_{\mathcal{S}_i}=M\right\}\sum_{k=1}^{M}\Pr\left\{M_A^{(i)}=k\right\}\\
&\quad\times\mathbb{E}_{\gamma_n^{(A,i)}|M_A^{(i)}}\left[\log_2(1+\gamma_n^{(A,i)})|M_A^{(i)}=k\right]\\
&=\sum_{M=1}^{\infty}\Pr\left\{M_{\mathcal{S}_i}=M\right\}\sum_{k=1}^{M}\binom{M}{k}P_r^{(A,i)^k}\left(1-P_r^{(A,i)}\right)^{M-k}\\
&\quad\times\log_2 e\int_0^\infty\frac{1-F_{\gamma_n^{(A,i)}|M_A^{(i)}}(\gamma|k)}{1+\gamma}\mathrm{d}\gamma,
\end{aligned}
\tag{17}
$$

where $\mathbb{E}_\alpha\{\cdot\}$ denotes the expectation operation with respect to random variable α, and $F_{\gamma_n^{(A,i)}|M_A^{(i)}}(\gamma|k)$ is the conditional cumulative distribution function (CDF) of $\gamma_n^{(A,i)}$ conditioned on the event that there are $M_A^{(i)}=k$ MSs in region A of cell i. The average spectral efficiency provided by cell i can be obtained as

$$
\overline{\eta}^{(i)}=N_C\overline{\eta}_n^{(C,i)}+N_E\overline{\eta}_n^{(E,i)}
\tag{18}
$$

and thus, the overall spectral efficiency of the network can be obtained as

$$
\overline{\eta}=\sum_{\forall i}\overline{\eta}^{(i)}=N_C\sum_{\forall i}\overline{\eta}_n^{(C,i)}+N_E\sum_{\forall i}\overline{\eta}_n^{(E,i)}.
\tag{19}
$$

Hence, now the problem is that of determining the conditional CDF $F_{\gamma_n^{(A,i)}|M_A^{(i)}}(\gamma|k)$ for each of the scheduling rules under analysis.

A. MSINR SCHEDULING

In each scheduling period and on each RB n in region A of cell i, the MSINR scheduler serves the MS experiencing the highest instantaneous SINR, that is,

$$
\gamma_n^{(A,i)}=\max_{u\in\mathcal{M}_A^{(i)}}\{\mathcal{M}_A^{(i)}\}.
\tag{20}
$$

According to this rule, the conditional CDF of $\gamma_n^{(A,i)}$, conditioned on the event that there are $M_A^{(i)}=k$ MSs in region A of cell i and on the sets $\boldsymbol{\pi}^A=\{\pi_{i,u}^A\}_{\forall u\in\mathcal{M}_A^{(i)}}$, $\boldsymbol{x}=\{x_u\}_{\forall u\in\mathcal{M}_A^{(i)}}$, $\boldsymbol{y}=\{y_u\}_{\forall u\in\mathcal{M}_A^{(i)}}$ and $\boldsymbol{\xi}=\{\xi_u\}_{\forall u\in\mathcal{M}_A^{(i)}}$, can be derived as

$$
\begin{aligned}
&F_{\gamma_n^{(A,i)}|M_A^{(i)},\boldsymbol{\pi}^A,\boldsymbol{x},\boldsymbol{y},\boldsymbol{\xi}}(\gamma|k,\boldsymbol{p},\boldsymbol{x},\boldsymbol{y},\boldsymbol{\xi})\\
&\qquad=\prod_{u\in\mathcal{M}_A^{(i)}}F_{\gamma_n^{(A,i)}|\pi_{i,u}^A,x_u,y_u,\xi_u}(\gamma|p_u,x_u,y_u,\xi_u).
\end{aligned}
\tag{21}
$$

Consequently, as on each RB n in region A of cell i the MSs are statistically equivalent in terms of SINR, the conditional CDF $F_{\gamma_n^{(A,i)}|M_A^{(i)}}(x|k)$ in (17) for the MSINR scheduling policy simplifies to

$$
F^{\mathrm{MSINR}}_{\gamma_n^{(A,i)}|M_A^{(i)}}(\gamma|k)=\left[F_{\gamma_n^{(A,i)}}(\gamma)\right]^k,
\tag{22}
$$

where the CDF of the instantaneous SINR $\gamma_{u,n}^{(A,i)}$ is

$$
\begin{aligned}
F_{\gamma_n^{(A,i)}}(\gamma)=\int_{-\infty}^{\infty}\iint_{(x,y)\in\mathcal{S}_i}\int_0^\infty&f_{\pi_{i,u}^A,x_u,y_u,\xi_u}(p,x,y,\xi)\\
&\times F_{\gamma_n^{(A,i)}|\pi_{i,u}^A,x_u,y_u,\xi_u}(\gamma|p,x,y,\xi)\mathrm{d}p\mathrm{d}x\mathrm{d}y\mathrm{d}\xi.
\end{aligned}
\tag{23}
$$

Note that this expression, as well as (12), can be straightforwardly evaluated using numerical integration tools, thus greatly reducing the time required to accurately compute these statistical functions when compared to Monte Carlo simulation-based strategies. In fact, it was found out that the computation time required to evaluate (12) and (23) was orders of magnitude lower than that required by the corresponding simulation approach.

B. RR SCHEDULING

A round-robin scheduler allocates RBs to MSs in a fair time-sharing approach. Since the SINRs experienced by MSs in region A of cell i on each RB n are statistically equivalent, serving $M_A^{(i)}=k$ MS using a RR scheduling policy is equivalent to serving $M_A^{(i)}=1$ MS with MSINR (even when MSs are selected with non uniform probability). Therefore, the conditional CDF in (17) simplifies, now, to

$$
F^{\mathrm{RR}}_{\gamma_n^{(A,i)}|M_A^{(i)}}(\gamma|k)=F^{\mathrm{MSINR}}_{\gamma_n^{(A,i)}|M_A^{(i)}}(\gamma|1)=F_{\gamma_n^{(A,i)}}(\gamma).
\tag{24}
$$

V. OPTIMAL DESIGNS

Let us define the FFR spectrum allocation factor as the quotient between the number of RBs allocated to cell-center MSs and the number of RBs allocated to cell-edge MSs, that is, $\rho \triangleq |\mathcal{F}_C| / |\mathcal{F}_E|$. Undoubtedly, the performance of the FFR-aided OFDMA-based irregular cellular network, in terms of spectral efficiency and throughput fairness among cell-center and cell-edge MSs, will be basically determined by the power thresholds used in each of the cells constituting the cellular network, as well as the FFR spectrum allocation factor adopted over the whole service area of the network. Hence, in this section we introduce some designs that, broadly speaking, aim at determining the set of power thresholds $\mathcal{P}_{th}^{*} = \left\{P_{th}^{(1)*}, \ldots, P_{th}^{(N_{\mathrm{BS}})*}\right\}$ and the spectrum allocation factor ρ^{*} maximizing the spectral efficiency while fulfilling operator-defined system constraints related to fairness. In particular, two optimization designs are explored: 1) the fixed spectrum allocation factor design (FxD) and 2) the QoS-constrained design (QoScD). The FxD aims at obtaining the set of power thresholds maximizing the spectral efficiency of a network for which the spectrum allocation factor has been fixed to $\rho = \rho_0$. The QoScD, instead, aims at determining both the set of power thresholds and the spectrum allocation factor that maximize the network spectral efficiency under the constraint that the cell-edge user's spectral efficiency is at least a fixed fraction q of the one achieved at the cell-center. We first introduced these designs in [15] but in the context of regular cellular networks without considering the effect of spatially correlated shadowing. In a regular cellular environment it is typically assumed that the network has an infinite geographical extension and consequently, that all the cells in the network are characterized by exactly the same performance. In such a simplified environment, the cellular network can be optimized by considering the behaviour of a single generic cell, thus greatly simplifying the whole optimization process. The complexity increase associated to the extension of the proposed optimization framework to the case of irregular cellular networks will largely depend on the selected optimization design.

A. FIXED SPECTRUM ALLOCATION FACTOR DESIGN

Adapting the FxD-based approach to the case of irregular cellular networks is quite straightforward (once the cell association and FFR-based user's classification processes have been statistically characterized) because, in this particular case, once the FFR spectrum allocation factor has been fixed to $\rho = \rho_0$, the optimal power threshold for BS i can be obtained irrespective of the power thresholds applied by the other BSs. That is, the FxD-based optimization problem, aiming at the spectral efficiency optimization of the network, can be split into N_{BS} cell optimization subproblems as

$$P_{th}^{(i)*} = \arg \max_{0 \le P_{th}^{(i)} < \infty} N_C \overline{\eta}_n^{(C,i)} + N_E \overline{\eta}_n^{(E,i)} \tag{25}$$

for all $i \in \{1, \ldots, N_{\mathrm{BS}}\}$. Notice that these optimization problems can be efficiently solved using standard software optimization packages (e.g., Matlab).

B. QoS CONSTRAINED DESIGN

In the QoScD-based approach, the FFR-related parameters are selected to warrant a prescribed trade-off between the spectral efficiency provided to cell-center MSs and that provided to MSs located in the cell-edge. In this case, the constrained optimization problem can be formulated in terms of the QoS factor q as

$$\left(\mathcal{P}_{th}^{*}, \rho^{*}\right) = \arg \max_{(\mathcal{P}_{th}, \rho)} N_C \sum_{\forall i} \overline{\eta}_n^{(C,i)} + N_E \sum_{\forall i} \overline{\eta}_n^{(E,i)}, \quad \text{subject to } N_E \overline{\eta}_n^{(E,i)} \ge q N_C \overline{\eta}_n^{(C,i)} \quad \forall i. \tag{26}$$

This problem can be easily solved in two simple steps. In the first step, an optimization subproblem equivalent to (26) is posed for each individual cell in the system. That is,

$$\left(P_{th}^{(i)\dagger}, \rho_i^{\dagger}\right) = \arg \max_{\left(P_{th}^{(i)}, \rho_i\right)} N_C \overline{\eta}_n^{(C,i)} + N_E \overline{\eta}_n^{(E,i)}, \quad \text{subject to } N_E \overline{\eta}_n^{(E,i)} \ge q N_C \overline{\eta}_n^{(C,i)} \tag{27}$$

for all $i \in \{1, \ldots, N_{\mathrm{BS}}\}$, where the superscript $(\cdot)^{\dagger}$ is used to indicate the optimal solutions to these subproblems. The smaller an FFR spectrum allocation factor is, the higher is the number of frequential resources allocated to the cell-edge and thus, the higher is the cell-edge throughput in comparisson to the cell-center one. Thus, once we have obtained the FFR spectrum allocation factors $\rho_i^{\dagger}$ for all $i \in \{1, \ldots, N_{\mathrm{BS}}\}$, the optimal FFR spectrum allocation factor fulfilling the constraint in problem (26) can be obtained as

$$\rho^{*} = \min_{i \in \{1, \ldots, N_{\mathrm{BS}}\}} \rho_i^{\dagger}. \tag{28}$$

Now, the set of optimal power thresholds $\mathcal{P}_{th}^{*} = \left\{P_{th}^{(1)*}, \ldots, P_{th}^{(N_{\mathrm{BS}})*}\right\}$ can be obtained in a second step by solving the FxD optimization problem (25) with $\rho = \rho^{*}$. Notice, again, that all these optimization problems can be efficiently solved using standard software optimization packages (e.g., Matlab).

VI. PERFORMANCE EVALUATION

In order to validate the proposed analytical framework, the network schematically shown in Fig. 1 is considered. For the sake of reproducibility, the locations of the 19 BSs for the particular scenario used in this work are listed in Table 1. Furthermore, the main system parameters used to generate both the analytical and simulation results, which are based on [23], are summarized in Table 2.

Results shown in Fig. 2 represent the CDF of the instantaneous SINR experienced by an arbitrary MS u located in either the cell-center or the cell-edge of different BSs and for different system setups. Figure 2a shows the CDF of the SINR experienced by MSs associated to BS 1 when $Q_c = 3$ and in scenarios subject to different degrees of shadow fading.

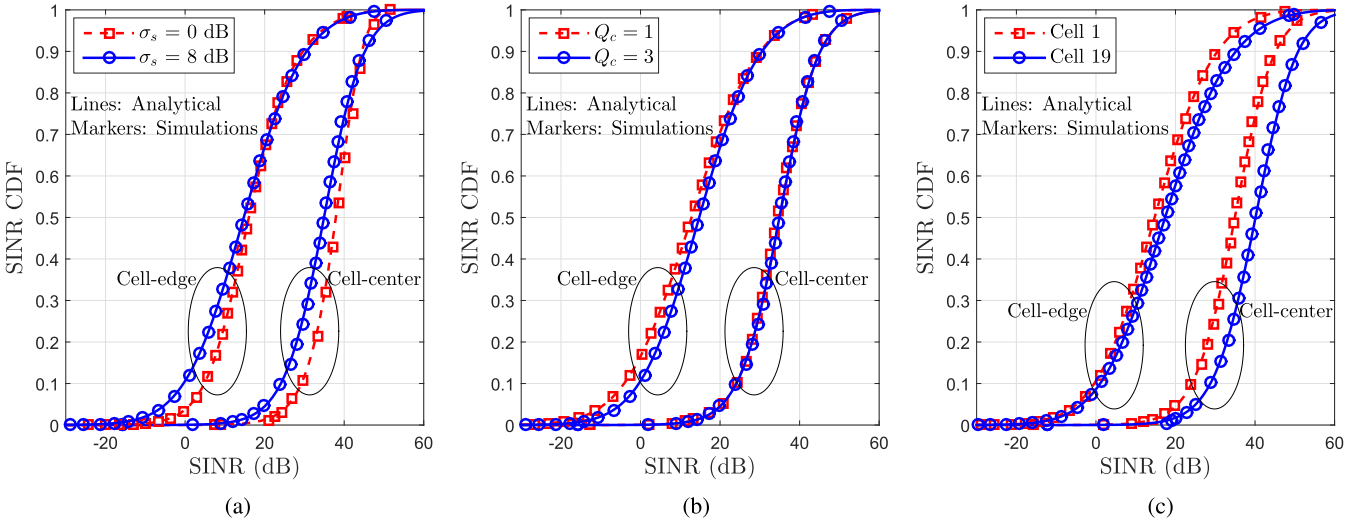

FIGURE 2. CDF of the SINR experienced by a MS in different cells and under different system setups with $P_{th}^{(i)} = -50$ dBm. (a) Cell 1, $Q_c = 3$. (b) Cell 1, $\sigma_s = 8$ dB. (c) BSs 1 & 19, $Q_c = 3$, $\sigma_s = 8$ dB.

TABLE 1. Location of the BSs.

Base station	$x^{(i)}$ (in meters)	$y^{(i)}$ (in meters)
BS 1	0	0
BS 2	637.5	1875
BS 3	-975	1725
BS 4	-937.5	1050
BS 5	-625	825
BS 6	750	750
BS 7	2062.5	412.5
BS 8	825	187.5
BS 9	-1750	75
BS 10	-720	-180
BS 11	1395	-225
BS 12	-1800	-862.5
BS 13	-1260	-975
BS 14	-900	-1117.5
BS 15	-225	-825
BS 16	600	-705
BS 17	975	-817.5
BS 18	1335	-1125
BS 19	2175	-712.5

TABLE 2. Network parameters.

System parameter	Value
Minimum distance among the BS and MSs	35 m
Antenna configuration	SISO
Transmit power of the BS	46 dBm
Antenna gain at the BS	14 dBi
Power spectral density of noise	-174 dBm/Hz
Receiver noise figure	7 dB
Total bandwidth	20 MHz
Subcarrier spacing	15 kHz
Occupied subcarriers	1200
Subcarriers per RB	12
Total number of resource blocks	100
Path loss model	$15.3 + 37.6 \log_{10}(d)$ dB
Small-scale fading model	Rayleigh channel
Shadowing model	Lognormal ($\epsilon = 0.5$)
Monte-Carlo trials	10,000

Fig. 2b compares the CDF of the SINR experienced by MSs located in BS 1 when either $Q_c = 1$ or $Q_c = 3$ and assuming a shadow fading with $\sigma_s = 8$ dB. Fig. 2c compares de behaviour of the CDF of the SINR experienced by MSs associated either to BS 1, located in the inner region of the network, or BS 19, located in the outer-region of the network, when $Q_c = 3$ and $\sigma_s = 8$ dB. Throughout this section, lines are used to represent analytical results and markers correspond to results obtained through Monte-Carlo simulations. The first point worth stressing is the very good match between analytical and simulation results, thus validating the analytical framework developed in Section III. Focusing now on performance issues, results presented in Fig. 2a indicate that, as expected, the SINR values experienced by MSs located in the cell-edge are considerably lower than those experienced by cell-center MSs. Furthermore, cellular scenarios subject to higher levels of spatially correlated shadow fading produce slightly lower values of SINR and with a higher statistical dispersion. As shown in Fig. 2b, MSs located in the cell-center are barely affected by the number of BSs involved in the cell association process. This is unsurprising because the cell-center MSs are located near the corresponding BS and consequently, it is highly probable that, irrespective of the value of Q_c, they associate to this BS. The cell-edge MSs, in contrast, are clearly benefitted by the use of a greater number of BSs involved in the cell association process because a cell-selection process limited to a low number of BSs decreases the probability of associating a given user to the most favourable BS (in the sense of maximizing the

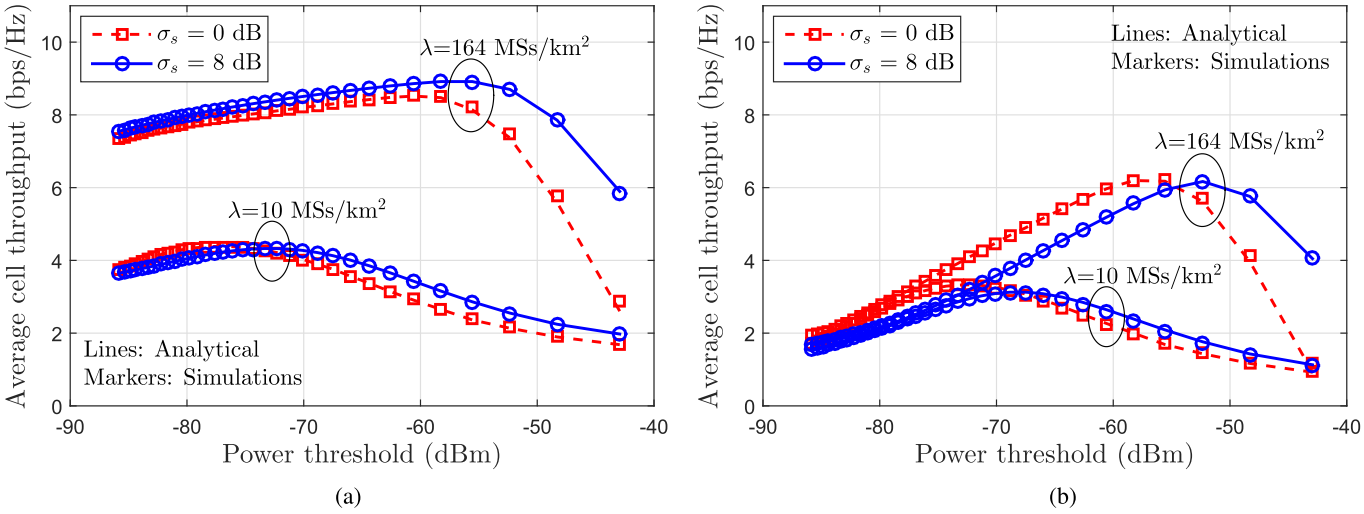

FIGURE 3. Average cell throughput versus power threshold in Cell 1 for different values of the normalized intensity λ and $Q_c = 3$ (FxD). (a) MSINR scheduler. (b) RR scheduler.

average SINR). Finally, results presented in Fig. 2c show that MSs located in different cells of the system are clearly affected by disparate levels of interference. In particular, MSs associated to interior cells of the network are observed to suffer from higher levels of interference eventually leading to lower levels of SINR when compared to MSs associated to MSs located in outer regions of the network.

A. FxD-BASED RESULTS

For the FxD-based approach, we have chosen to set the number of RBs allocated to the cell-center and cell-edge equal to 52 and 16, respectively, which are values typically used for this design [12], [14]. That is, the spectrum allocation factor has been set to $\rho = \rho_0 = 3.25$. Using this setup, Fig. 3 presents the average cell throughput provided by BS 1 as a function of the power threshold $P_{th}^{(1)}$. Illustrating the system behaviour under different network deployments, analytical and simulation results are shown for the RR and MSINR scheduling policies using two different values of the normalized intensity λ and two distinct levels of shadow fading. Again, it is worth noting the good agreement between the simulated and analytical results, hence validating in this case the analytical framework developed in Section IV. The average throughput increases with the average number of MSs per cell. This is basically due to two distinct causes. The first one, only exploited by the MSINR scheduling rule, is originated by the larger degree of multiuser diversity provided by the increase of λ. The second cause, specially significant for the RR scheduler, is that the increase of the average number of MSs per cell invariably decreases the probabilities of ending up with unpopulated cell-center and/or cell-edge regions to which nevertheless RBs are allocated, hence increasing the probability of properly exploiting the assigned RBs and avoiding the waste of resources.

A noteworthy effect, common to both scheduling rules, as it can be appreciated in Figs. 3a and 3b, is the shift of the optimal operating points of the FFR power threshold towards larger values when the shadowing standard deviations increases. This is indicative that the greater dispersion of SINRs caused by shadowing (already apparent in Fig. 2a) leads to a shrinkage of the central regions. Also, note that the optimal power thresholds for the MSINR scheduler are somewhat lower than the RR counterparts. That is, the central regions when using MSINR tend to be slightly greater than when using RR.

Once again, different irregular cells from the same network, namely cells 1 and 19, are considered in Fig. 4. The number of BSs involved in the cell association process is introduced as a parameter in Figs. 4a and 4b where the average cell-edge throughput for MSINR and RR scheduling policies is represented. As already noted, increasing Q_c yields better edge throughput results. Remarkably, this improvement is more visible in networks using an RR scheduler than in those using MSINR. This can be attributed to the fact that under RR the random user selection is more prone to schedule edge-MSs that are far from the BS and thus, more likely to be wrongly associated when using $Q_c = 1$. In contrast, when using MSINR the scheduled edge-MSs tend to be located close to the central-region border and hence, it is more likely that they are associated to the most favourable BS irrespective of the value of Q_c. Moreover, inner BSs (e.g., BS 1), suffering higher levels of inter-cell interference, attain lower edge throughput than outer BSs (e.g., BS 19). This phenomenon becomes even more exacerbated when considering the average cell throughput, as depicted in Fig. 4c, where the throughput provided by BSs 1 and 19 is shown for the case in which $Q_c = 3$ and assuming the use of both MSINR and RR scheduling rules.

Figure 5 shows the optimum overall network throughput under the FxD strategy as a function of the normalized intensity λ and spectrum allocation factor ρ for both MSINR and RR. Note that these results have been obtained by indi-

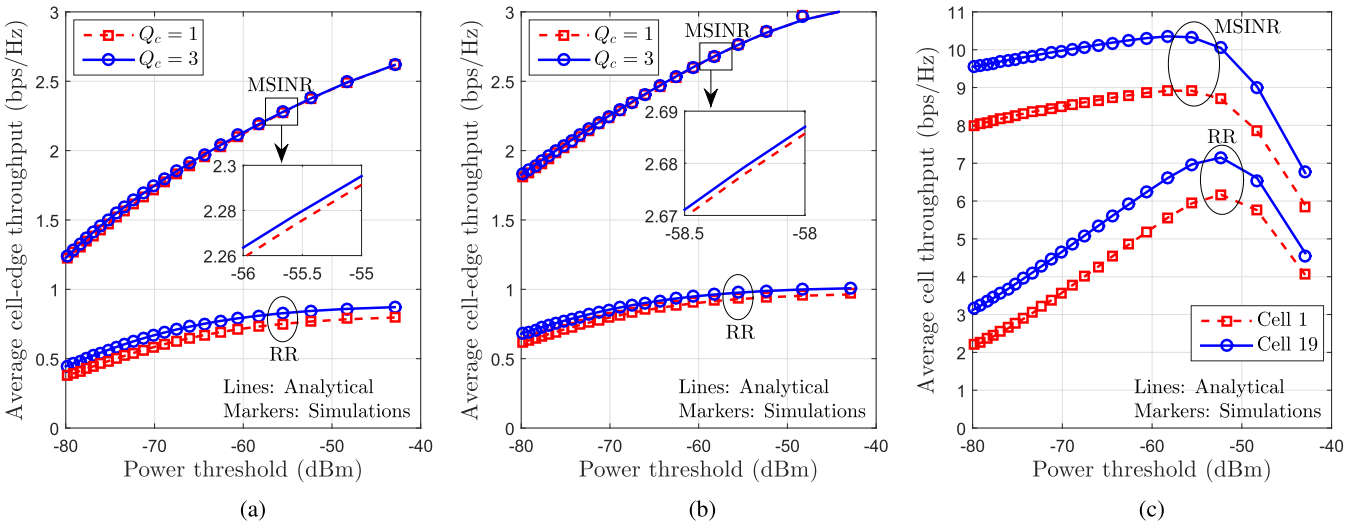

FIGURE 4. Average throughput versus power threshold in different irregular cells, $\sigma_s = 8$ dB, $\lambda = 164$ MSs/km^2 (FxD). (a) Cell 1. (b) Cell 19. (c) Cells 1 and 19, $Q_c = 3$.

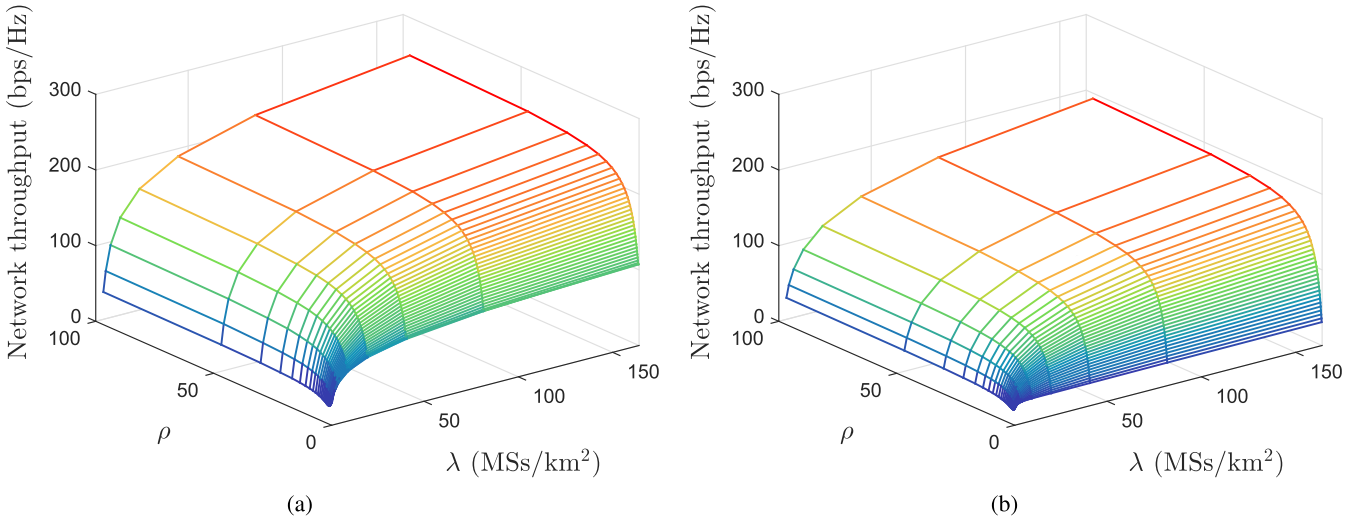

FIGURE 5. Network throughput, considering the optimal power thresholds $P_{th}^{(i)*}$ in all cells, as a function of both the normalized intensity λ and the spectrum allocation factor ρ, $Q_c = 3$, $\sigma_s = 8$ dB (FxD). (a) MSINR scheduler. (b) RR scheduler.

vidually solving the optimization problem in (25) for each of the 19 cells in the network. As it has already been commented, MSINR offers better performance thanks to the exploitation of multiuser diversity, notwithstanding that both MSINR and RR also benefit from having more MSs in the system thus diminishing the probability of having unpopulated regions. Note also that, irrespective of the scheduler in use and the normalized intensity λ, the higher the number of RBs allocated to the cell-center MSs the higher the network throughput. This is because, since the FxD approach does not enforce any constraint on fairness among cell-center and cell-edge MSs, the best strategy is to allocate as many resources as possible to those MSs that make the most of them, which invariably happen to be the central ones.

B. QoScD-BASED RESULTS

To assess the performance of the QoScD strategy under different QoS constraints, analytical and simulated network cell-center, cell-edge and overall throughputs as a function of the normalized intensity λ are shown in Fig. 6 for both MSINR and RR schedulers. Two different quality factors, $q = 0.02$ and $q = 0.2$, have been considered, corresponding to low and high throughput fairness requirements between cell-centre and cell-edge MSs. Again, it is worth noting the good agreement between the simulated and analytical results. Also note that these results have been generated using the optimal solution of the QoScD approach, that is, they have been obtained using the optimal spectrum allocation factor ρ^* and the optimal power thresholds $\mathcal{P}_{th}^* = \left\{P_{th}^{(1)*}, \ldots, P_{th}^{(19)*}\right\}$.

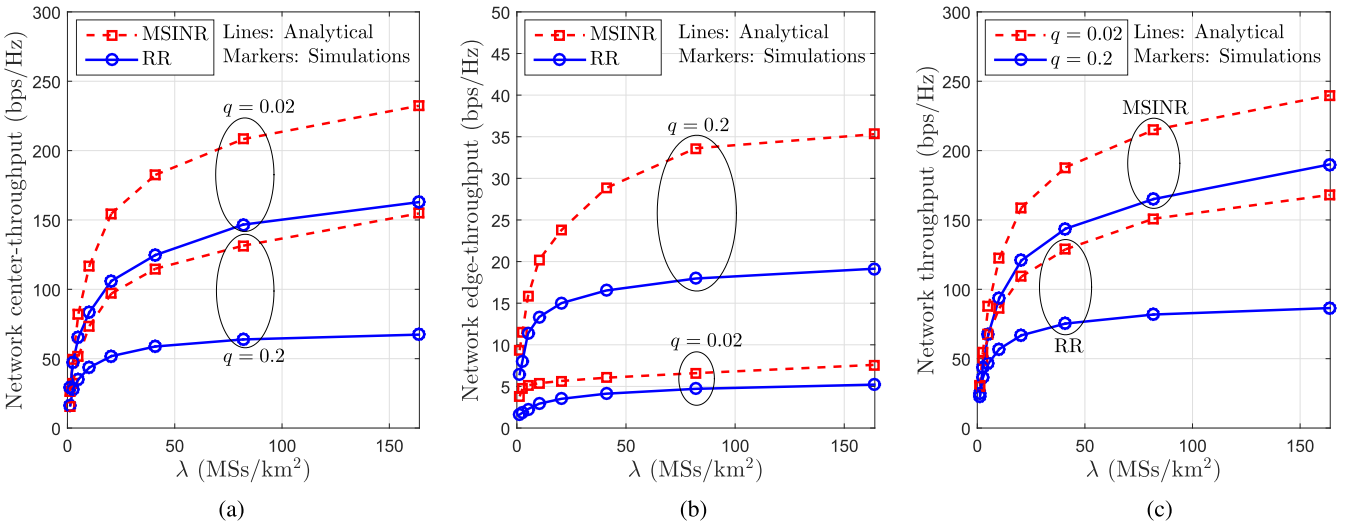

FIGURE 6. Network cell-center, cell-edge and overall throughputs versus normalized intensity λ for both MSINR and RR schedulers under different QoS constraints q ($\sigma_s = 8$ dB, $Q_c = 3$, QoScD). (a) Network cell-center throughput. (b) Network cell-edge throughput. (c) Overall network throughput.

As in the FxD-based FFR design, the MSINR scheduler provides a clear average throughput performance advantage when compared to the RR scheduler owing to the optimal exploitation of multiuser diversity. Remarkably, the parameter q is seen to effectively act as a knob to trade cell-edge and cell-center performance. In particular, note how the network center-throughput (see Fig. 6a) for $q = 0.02$ is much higher than for $q = 0.2$. Conversely, the network edge-throughput behaves the other way round (see Fig. 6b), that is, increasing q leads to a throughput improvement in that region. Therefore, increasing the QoS requirement q enforces a higher degree of fairness between cell-centre and cell-edge MSs at the cost of decreasing the average network throughput as it can clearly be appreciated in Fig. 6c. In fact, the QoScD strategy causes the system to gravitate away from the full spectrum reuse strategy since increasing the QoS requirement q increases the amount of resources allocated to the cell-edge MSs.

In order to make further apparent the consequences of the network topology irregularity, Fig. 7 presents the average throughput provided by BSs 1 and 19 as a function of the normalized intensity λ for both MSINR and RR schedulers and using $q = 0.2$, $\sigma_s = 8$ dB and $Qc = 3$. As in the FxD approach, Cell 19 attains higher throughput values owing to the reduced levels of interference experienced by MSs located in the outer regions of the cellular network. MSs associated to Cell 1, in contrast, which are located in the inner regions of the network, are subject to higher levels of inter-cell interference causing a drop in cell throughput.

To gain a more complete understanding of the effects the QoScD approach has on the network performance, Figure 8 shows the optimal overall network throughput as a function of both the normalized intensity λ and the QoS factor q for both MSINR and RR scheduling rules. It can be observed that the most important sacrifice in terms of overall network

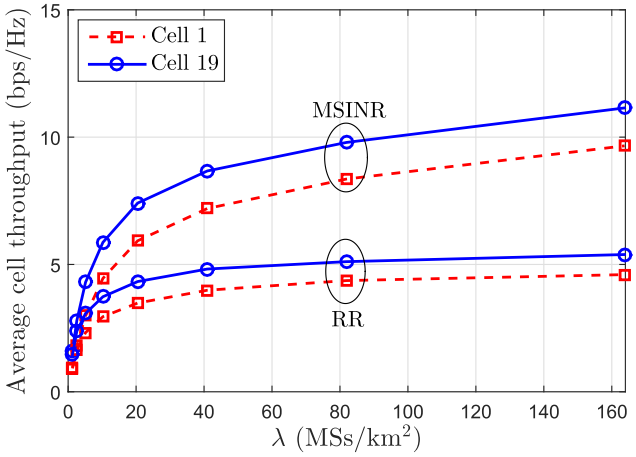

FIGURE 7. Average cell throughput provided by BS 1 and BS 19 versus normalized intensity λ for both MSINR and RR schedulers under different QoS constraints q ($q = 0.2$, $\sigma_s = 8$ dB, $Q_c = 3$, QoScD).

throughput happens when transiting from a situation in which no QoS fairness constraints are enforced ($q = 0$) to setups where loose fairness restrictions are introduced ($q < 0.15$). In contrast, note that, irrespective of λ, the sensitivity of the network throughput to values of q greater than 0.3 is rather mild thus indicating that for values beyond $q = 0.3$ the fairness between cell-center and cell-edge MSs can be increased without an exceedingly large incremental cost in terms of overall network throughput. Again, note that increasing λ invariably results in network throughput improvements that, in the case of RR are solely due to the reduced probability of having unpopulated cell regions, whereas in the case of MSINR are also motivated by the increase of multiuser diversity.

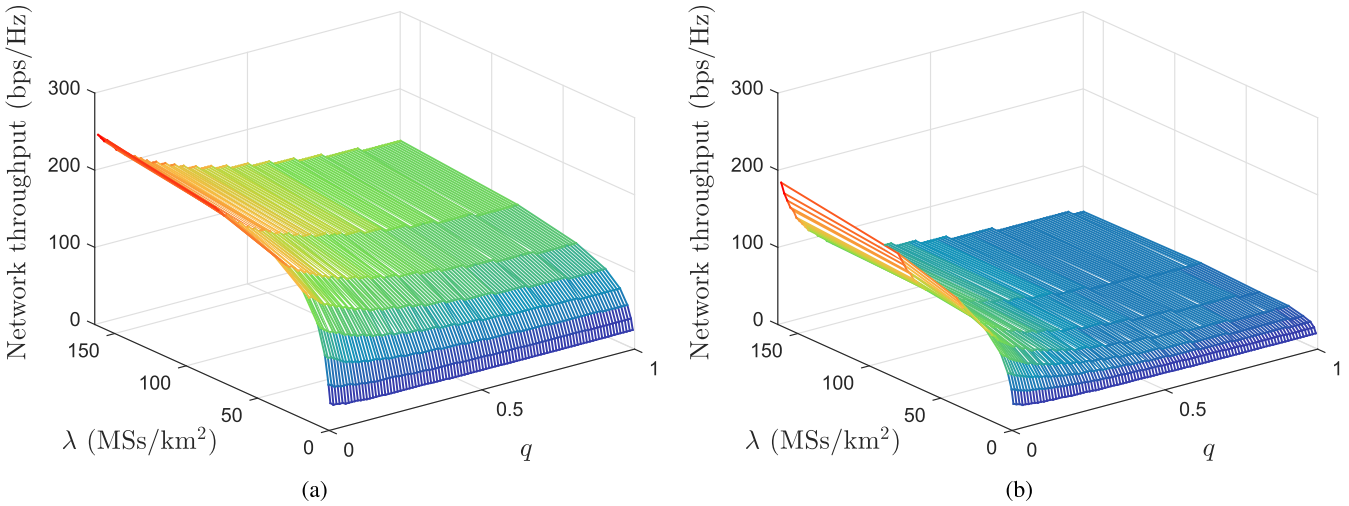

FIGURE 8. Optimal overall network throughput (considering the optimal spectrum allocation factor ρ^* and the optimal power thresholds $P_{th}^{(i)*}$ in all cells) as a function of both the QoS factor q and the normalized intensity λ ($Q_c = 3$, $\sigma_s = 8$ dB, QoScD). (a) MSINR scheduler. (b) RR scheduler.

VII. CONCLUSION

This paper has presented and validated a novel analytical framework to evaluate the performance of FFR-aided OFDMA-based multi-cellular networks subject to correlated shadowing and with an irregular BS deployment. In this scenario, the cell association process and the partition of each cell into edge and center regions are critical aspects and they have both been incorporated to the derivation of a mathematically tractable statistical characterization of the instantaneous SINR experienced by any user in any of the irregular cells in the network. Furthermore, these expressions have been particularized to the specific case of two popular scheduling rules, namely, RR and MSINR. The resulting distribution functions for the instantaneous SINR have then been used to derive the average throughput of both the whole network and of each individual cell, which in turn allowed the formulation of designs with different restrictions from which the optimal FFR parameters can be derived.

In particular, two optimization designs, namely, the fixed spectrum allocation factor (FxD) and the QoS constrained (QoScD) designs, have been proposed and thoroughly explored. The simple FxD-based FFR design has been shown to provide very high levels of network spectral efficiency at the cost of loosing fairness between cell-center and cell-edge MSs. In contrast, the more elaborated QoScD-based FFR design, has been shown to allow network operators to enforce any desired minimum degree of throughput fairness between cell-center and cell-edge MSs while, at the same time, minimizing the sacrifice of overall network throughput. Irrespective of the optimization design, it has been shown that increasing the average number of MSs per cell invariably leads to a throughput increase. This is basically due to that, first, using a channel-aware scheduler enables exploiting the multiuser diversity and, second, because increasing the average number of MSs per cell reduces the probability of ending up with unpopulated cell-center and/or cell-edge regions. Another result worth stressing is that, irrespective of either the optimization design or the scheduling rule, increasing the number of BSs involved in the cell association process always leads to network performance improvements, specially for cell-edge MSs, more likely to be wrongly associated to an inappropriate BS. It has also been proved that shadowing plays an important role when optimizing FFR-aided OFDMA-based designs.

Further work will concentrate on extending the analysis so as to encompass heterogeneous OFDMA-based networks, non-uniform distributions of MSs and the use of more sophisticated ICIC techniques (e.g., soft/adaptive frequency reuse, network MIMO).

REFERENCES

[1] E. Dahlman, S. Parkvall, and J. Skold, *4G: LTE/LTE-Advanced for Mobile Broadband*, 2nd ed. Amsterdam, The Netherlands: Elsevier, 2013.

[2] A. S. Hamza, S. S. Khalifa, H. S. Hamza, and K. Elsayed, "A survey on inter-cell interference coordination techniques in OFDMA-based cellular networks," *IEEE Commun. Surveys Tuts.*, vol. 15, no. 4, pp. 1642–1670, 4th Quart., 2013.

[3] N. Saquib, E. Hossain, and D. I. Kim, "Fractional frequency reuse for interference management in LTE-advanced hetnets," *IEEE Wireless Commun.*, vol. 20, no. 2, pp. 113–122, Apr. 2013.

[4] R. Knopp and P. A. Humblet, "Information capacity and power control in single-cell multiuser communications," in *Proc. IEEE Int. Conf. Commun. (ICC)*, vol. 1. Jun. 1995, pp. 331–335.

[5] B. Pijcke, M. Gazalet, M. Zwingelstein-Colin, and F.-X. Coudoux, "An accurate performance analysis of an FFR scheme in the downlink of cellular systems under large-shadowing effect," *EURASIP J. Wireless Commun. Netw.*, vol. 2013, no. 1, pp. 1–14, 2013.

[6] T. Novlan, R. Ganti, A. Ghosh, and J. Andrews, "Analytical evaluation of fractional frequency reuse for OFDMA cellular networks," *IEEE Trans. Wireless Commun.*, vol. 10, no. 12, pp. 4294–4305, Dec. 2011.

[7] H. Elsawy, E. Hossain, and M. Haenggi, "Stochastic geometry for modeling, analysis, and design of multi-tier and cognitive cellular wireless networks: A survey," *IEEE Commun. Surveys Tuts.*, vol. 15, no. 3, pp. 996–1019, 3rd Quart., 2013.

[8] J.-M. Kelif, S. Senecal, M. Coupechoux, and C. Bridon, "Analytical performance model for Poisson wireless networks with pathloss and shadowing propagation," in *Proc. IEEE Globecom Workshops (GC Wkshps)*, Dec. 2014, pp. 1528–1532.

[9] F. Baccelli and X. Zhang, "A correlated shadowing model for urban wireless networks," in *Proc. IEEE Conf. Comput. Commun. (INFOCOM)*, Apr. 2015, pp. 801–809.
[10] M. Assaad, "Optimal fractional frequency reuse (FFR) in multicellular OFDMA system," in *Proc. IEEE 68th Veh. Technol. Conf. (VTC-Fall)*, Sep. 2008, pp. 1–5.
[11] A. Najjar, N. Hamdi, and A. Bouallegue, "Efficient frequency reuse scheme for multi-cell OFDMA systems," in *Proc. IEEE Symp. Comput. Commun. (ISCC)*, Jul. 2009, pp. 261–265.
[12] Z. Xu, G. Y. Li, C. Yang, and X. Zhu, "Throughput and optimal threshold for FFR schemes in OFDMA cellular networks," *IEEE Trans. Wireless Commun.*, vol. 11, no. 8, pp. 2776–2785, Aug. 2012.
[13] G. Femenias and F. Riera-Palou, "Corrections to and comments on 'throughput and optimal threshold for FFR schemes in OFDMA cellular networks,'" *IEEE Trans. Wireless Commun.*, vol. 14, no. 5, pp. 2926–2928, May 2015.
[14] J. García-Morales, G. Femenias, and F. Riera-Palou, "Multi-layer FFR-aided OFDMA-based networks using channel-aware schedulers," *Mobile Netw. Appl.*, vol. 22, no. 6, pp. 1068–1082, 2016.
[15] J. García-Morales, G. Femenias, and F. Riera-Palou, "Analysis and optimization of FFR-aided OFDMA-based heterogeneous cellular networks," *IEEE Access*, vol. 4, pp. 5111–5127, 2016.
[16] A. Mahmud and K. A. Hamdi, "A unified framework for the analysis of fractional frequency reuse techniques," *IEEE Trans. Wireless Commun.*, vol. 62, no. 10, pp. 3692–3705, Oct. 2014.
[17] A. M. Alam, P. Mary, J.-Y. Baudais, and X. Lagrange, "Energy efficiency-spectral efficiency tradeoff in interference-limited wireless networks with shadowing," in *Proc. IEEE 82nd Veh. Technol. Conf. (VTC Fall)*, Sep. 2015, pp. 1–5.
[18] G. Femenias and L. Carrasco, "Effect of slow power control error on the reverse link of OSTBC DS-CDMA in a cellular system with Nakagami frequency-selective MIMO fading," *IEEE Trans. Veh. Technol.*, vol. 55, no. 6, pp. 1927–1934, Nov. 2006.
[19] A. J. Viterbi, A. M. Viterbi, K. S. Gilhousen, and E. Zehavi, "Soft handoff extends CDMA cell coverage and increases reverse link capacity," *IEEE J. Sel. Areas Commun.*, vol. 12, no. 8, pp. 1281–1288, Oct. 1994.
[20] "Evolved universal terrestrial radio access (E-UTRA); Further advancements for E-UTRA physical layer aspects," 3GPP, Tech. Specification Group (TSG) Radio Access Netw., Los Angeles, CA, Tech. Rep. 36.814 v9.0.0, 2010.
[21] G. L. Stüber, *Principles of Mobile Communications* 2nd ed. Norwell, MA, USA: Kluwer, 2001.
[22] M. Abramowitz and I. A. Stegun, *Handbook of Mathematical Functions: With Formulas, Graphs, and Mathematical Tables*, vol. 55. North Chelmsford, MA, USA: Courier Corporation, 1964.
[23] *Home Enode B (HeNB) Radio Frequency (RF) Requirements Analysis (Release 9)*, document TR36.921, v9.0.0. 2010.

JAN GARCÍA-MORALES (S'14) was born in Cienfuegos, Cuba, in 1984. He received the degree in telecommunications and electronics from the Faculty of Electrical Engineering, Central University of Las Villas, Villa Clara, Cuba, in 2008, and the M.Sc. degree in information technologies from the Department of Mathematics and Informatics, University of the Balearic Islands, in 2013, where he is currently pursuing the Ph.D. degree in the information and communication technologies. From 2008 to 2012, he was with the Mobile Telecommunications Company Movitel S.A. He was with Innovation and Technology Company IBITEC S.L., as a Santander-Crue-Cepyme Internship Researcher Assistant conducting research in designing and programming automatic systems and sensor networks. Motivated by the research in the telecommunications and information technology area, he applied for one of the Santander-Iberoamerica Scholarship in 2012 to enroll in the master's degree (research itinerary) in Spain. In 2013, he received a pre-doctoral scholarship from the Conselleria d'Educació, Cultura i Universitats (Govern de les Illes Balears) under Grant FPI/1538/2013 as part of an operational program co-financed by the European Social Fund. He is member of the Mobile Communications Group.

GUILLEM FEMENIAS (SM'11) received the Telecommunication Engineer degree and the Ph.D. degree in electrical engineering from the Technical University of Catalonia (UPC), Barcelona, Spain, in 1987 and 1991, respectively. From 1987 to 1994, he was a Researcher with UPC, where he became an Associate Professor in 1992. In 1995, he joined the Department of Mathematics and Informatics, University of the Balearic Islands (UIB), Mallorca, Spain, where he also became a Full Professor in 2010. He is currently leading the Mobile Communications Group, UIB, where he has been the Project Manager of Projects ARAMIS, DREAMS, DARWIN, MARIMBA, COSMOS, ELISA, and TERESA, and all of them were funded by the Spanish and Balearic Islands Governments. He was also involved with several European Projects, such as ATDMA, CODIT, and COST. His current research interests and activities span the fields of digital communications theory and wireless communication systems, with particular emphasis on cross-layer transceiver design, resource management, and scheduling strategies applied to fourth- and fifth-generation wireless networks. On these topics, he has published over 90 journal and conference papers, and some book chapters. He was the recipient of the Best Paper Awards at the 2007 IFIP International Conference on *Personal Wireless Communications* and at the 2009 IEEE Vehicular Technology Conference-Spring. He has served for the various IEEE conferences as a Technical Program Committee Member, as the Publications Chair for the IEEE 69th Vehicular Technology Conference (VTC-Spring 2009) and as Local Organizing Committee member of the IEEE Statistical Signal Processing.

FELIP RIERA-PALOU (SM'11) received the B.S. and M.S. degrees in computer engineering from the University of the Balearic Islands (UIB), Mallorca, Spain, in 1997, the M.Sc. and Ph.D. degrees in communication engineering from the University of Bradford, U.K., in 1998 and 2002, respectively, and the M.Sc. degree in statistics from the University of Sheffield, U.K., in 2006. From 2002 to 2005, he was with the Philips Research Laboratories, Eindhoven, The Netherlands, first as a Marie Curie Post-Doctoral Fellow (European Union) and then as a member of Technical Staff. He was involved in research programs related to wideband speech/audio compression and speech enhancement for mobile telephony with the Philips Research Laboratories. From 2005 to 2009, he was a Research Associate, Ramon y Cajal Program, Spanish Ministry of Science in the Mobile Communications Group, Department of Mathematics and Informatics, UIB. Since 2010, he has been an Associate Research Professor (I3 program, Spanish Ministry of Education), UIB. His current research interests are in the general areas of signal processing and wireless communications.